CONF-790125--67

MASTER

THE EFFECT OF DOSE ON THE EVOLUTION OF CAVITIES IN 500-KeV $^4He^+$-ION IRRADIATED NICKEL

by

G. Fenske, S. K. Das, M. Kaminsky, and G. H. Miley

Prepared for

The First Topical Meeting on Fusion Reactor Materials

Miami Beach, Florida

January 29-31, 1979

U of C-AUA-USDOE

ARGONNE NATIONAL LABORATORY, ARGONNE, ILLINOIS

Operated under Contract W-31-109-Eng-38 for the

U. S. DEPARTMENT OF ENERGY

Accepted for Publication in Journal of Nuclear Materials

THE EFFECT OF DOSE ON THE EVOLUTION OF CAVITIES IN 500-keV $^4He^+$-ION IRRADIATED NICKEL

G. FENSKE, S. K. DAS and M. KAMINSKY

Argonne National Laboratory, Argonne, Illinois 60439

G. H. MILEY

University of Illinois, Urbana, Illinois 61801

Transmission electron microscopy has been used to investigate the effect of total dose on the depth distribution of cavities (voids or bubbles) in nickel irradiated at 500°C with 500-keV $^4He^+$ ions. A transverse sectioning technique, which allows one to obtain the entire depth distribution of cavities and of damage from a single specimen, was utilized. The size, number density and volume fraction of bubbles or voids were measured from the micrographs taken from samples sectioned parallel to the direction of the incident beam. The results for the dose range studied (2×10^{19} to 1×10^{21} ions/m^2) show that the average cavity diameter, number density, and the volume fraction (i.e. swelling) increases with increasing dose. The peak in the swelling distribution occurs at depths 8 to 15% deeper than the peak in the calculated projected range profile.

1. INTRODUCTION

While radiation blistering phenomena have been widely studied, the mechanism of blister formation is still not fully understood [1]. Studies on the depth distribution of dislocation damage and of cavities (voids or bubbles) in ion irradiated metals are of great importance in understanding the blistering mechanism and the physics of particle penetration in solids. The changes in surface topography due to blistering has been widely investigated using scanning electron microscopy (SEM). However, only a few investigations [2-5] have been made using transmission electron microscopy (TEM) to observe changes in the microstructure of helium implanted regions. Of the TEM investigations cited above, only those by Ehrlich and Kaletta [4] have attempted to determine the depth distributions of the size, number density, or volume fraction of bubbles (swelling)—parameters that are important for an understanding of the blistering mechanism. The aim of the present study is to determine how the size, density and swelling change as a function of dose during the initial stages of bubble formation. The evaluation of data taken at higher doses is in progress and will be presented elsewhere.

2. EXPERIMENTAL TECHNIQUES

Polycrystalline nickel foils (∿ 50 μm thick) of 99.995% purity (Marz grade) were obtained from Material Research Corporation. The foils were first metallographically polished, then annealed at 900°C for two hours in a vacuum of ∿ 2.7×10^{-5} Pa and finally electropolished in a solution containing 140 ml phosphoric acid, 10 ml H_2SO_4, 43 ml H_2O and 2 g chromium trioxide. The targets were irradiated at 500°C in a vacuum of ∿ 1.3×10^{-5} Pa with 500-keV $^4He^+$ ions. The irradiated foils were first lightly sputter cleaned with 2-keV Ar^+ ions, then given a nickel strike and finally electroplated with nickel. The electroplated samples were then sectioned parallel to the direction of the incident beam and 3 mm discs were spark cut from them. Thin foils suitable for TEM were prepared by electrolytic jet polishing. This transverse sectioning technique whose details are described elsewhere [5] allows one to study the entire depth distribution of bubbles from a single specimen. Some similar techniques have been used to study the depth distribution of damage [6] and of voids [7,8,9] but for helium gas bubbles, only conventional techniques have been used [4].

3. RESULTS

Figures 1(a) and 1(b) show typical bright field micrographs of the cavity and dislocation microstructures of nickel foils implanted with 500-keV $^4He^+$ ions to a dose of 1×10^{21} ions/m^2. The interface between the plating and the irradiated regions is clearly seen in these figures together with the cavities and dislocation damage. Fig.1(a) shows a cavity-denuded-zone extending to a depth of ∿ 0.15 to 0.2 μm from the interface. A similar trend was also observed for the lower doses ranging from 2×10^{19} to 1×10^{21} ions/m^2. A large fraction of the cavities appear to have been heterogeneously nucleated at or near dislocations. This heterogeneous nucleation could be observed more readily for the lower dose range mentioned above. Similar results have been observed by Harbottle [10] for neutron irradiated nickel, and by Laidler and Garner [11] for neutron irradiated, annealed 316 stainless steel. The cavities seen at the interface and in the plating (see Fig. 1(a)) are probably trapped hydrogen bubbles generated when the nickel strike was applied. It is

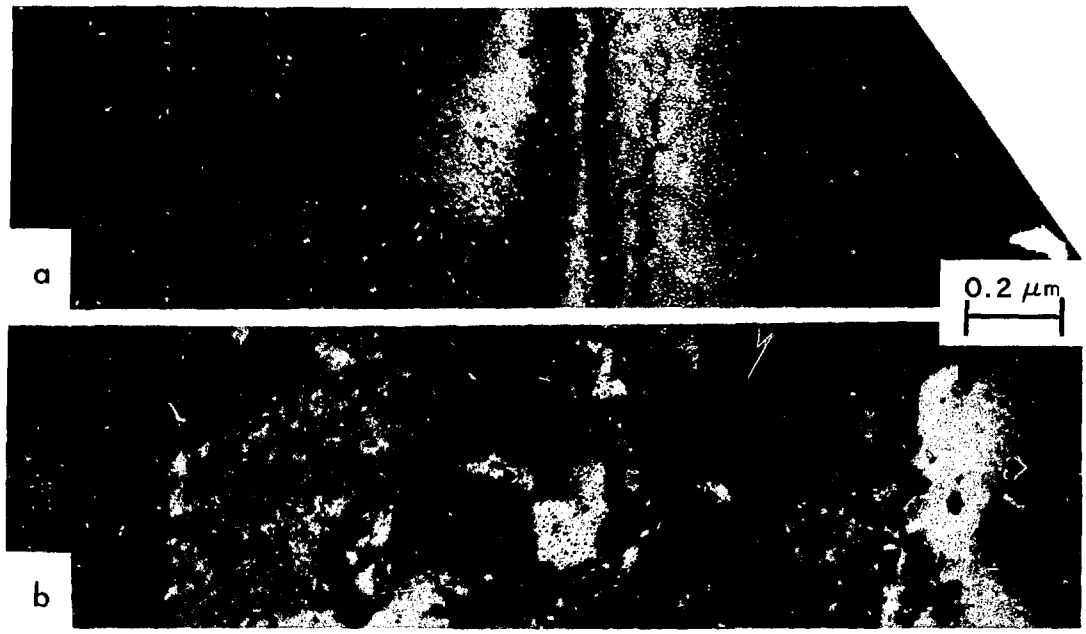

Figure 1: The (a) cavity and (b) dislocation microstructure of nickel irradiated with 500 keV $^4He^+$ ions at 500°C to a dose of 1 x 10^{21} ions/m^2.

important to note that these bubbles do not affect the cavity microstructure generated in the helium implanted region [5].

The dislocation microstructure near the peak in the damage (Fig. 1(b)) consists of dense dislocation tangles with a few dislocations extending towards the interface. At depths beyond the peak, the dislocation density decreases more rapidly than the density in regions located between the interface and the peak. Figs. 2(a)-2(d) show bright field micrographs of the cavities near the peak damage region of nickel irradiated at 500°C with 500-keV $^4He^+$ ions to total doses ranging from 2 x 10^{19} to 1 x 10^{21} ions/m^2. Here, the increase in the cavity diameter and in the number density with increasing dose can be clearly seen.

Figs. 3(a)-3(d) show quantitative results on the variations in the average cavity diameter and number density, and in the swelling due to cavities as a function of depth for nickel implanted at 500°C with 500-keV $^4He^+$ ions, for doses ranging from 2 x 10^{19} ions/m^2 to 1 x 10^{21} ions/m^2. For the lowest dose, 2 x 10^{19} ions/m^2, examined, the average size is nearly independent of depth (within an experimental accuracy of ± 0.5 nm). However, as the dose is increased above 2 x 10^{19} ions/m^2, the size is no longer independent of depth. For doses above 1 x 10^{20} ions/m^2, it is observed that the diameters are largest near the surface. For the highest dose of 1 x 10^{21} ions/m^2 the size distribution becomes bimodal with a second peak occurring at a depth of ∿1.15 μm, as shown in Fig.2(d). Near the surface, the volume fraction increases slowly with increasing depth, it then increases rapidly beyond ∿ 0.8 μm to maximum values between depths of ∿ 1.07 to ∿ 1.2 μm, and then it drops off rapidly to zero at depths beyond ∿ 1.4 to 1.5 μm. The solid and dashed curves in Figs. 3(a)-3(d) show the depth distributions of the energy deposited into damage and of the projected range, respectively. These distributions were computed using Brice's [12] computer programs: COREL, RASE4 and DAMG2 with theoretical LSS electronic stopping [13]. Comparing the swelling distribution with the theoretical range profiles in Figs. 3(a)-3(d), it is seen that the maximum swelling occurs at depths 8 to 15% deeper than the peak in the projected range profile. It may be pointed out that the results presented here are slightly different from preliminary results for 500-keV $^4He^+$ in nickel [14,15] given earlier, which had larger uncertainties in the location of the irradiated surface.

Values of the average size, number density and volume fraction at depths where the swelling is a maximum, are given in Table 1 for the data shown in Figs. 3(a)-3(d). From this table, it is seen that for doses up to 5 x 10^{20}/m^2 the increase in the volume swelling is predominantly due to the increase in the number density. Beyond a dose of 5 x 10^{20} ions/m^2 the increase

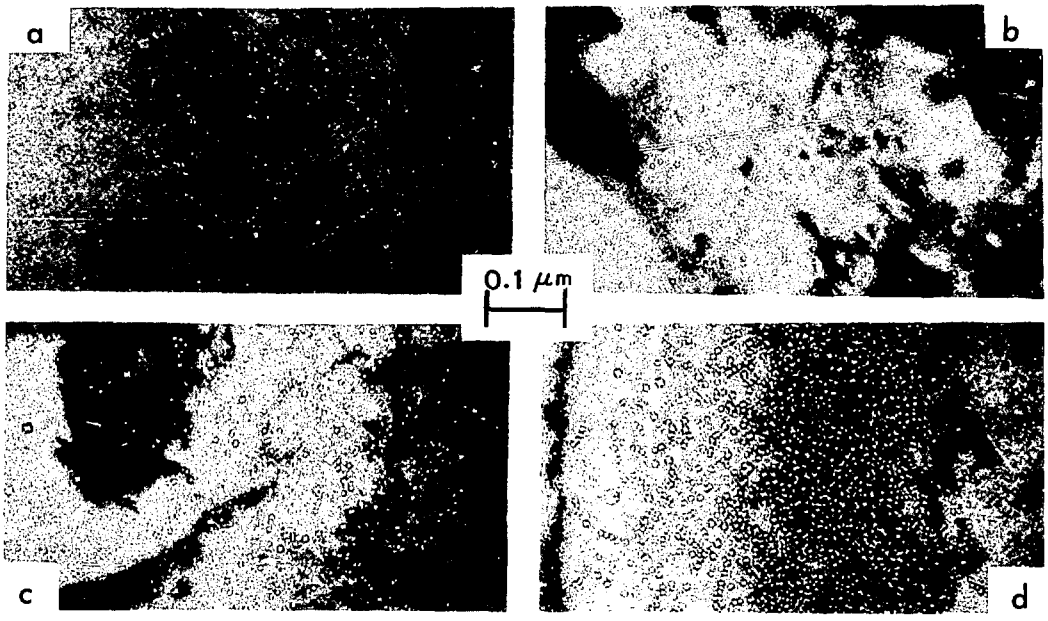

Figure 2: The cavity microstructure near the peak swelling depths for nickel irradiated with 500 keV $^4He^+$ ions at 500°C to doses of: (a) 2 x 10^{19} ions/m^2, (b) 1 x 10^{20} ions/m^2, (c) 5 x 10^{20} ions/m^2 and (d) 1 x 10^{21} ions/m^2.

in the volume swelling is now largely due to an increase in the size, rather than the increase in the number density. It should be noted that the micrographs in Figs. 2(a)-2(d) are not from TEM foils of the same thickness, thus the density of cavities may not be in the same relative proportion as those listed in Table 1.

4. DISCUSSION

An important result of the data presented here is that the peak swelling occurs at depths ∿ 8 to 15% deeper than the peak in the calculated projected range profile, or 15 to 25% deeper than the peak in the profile of the calculated energy deposited into damage. These theoretical profiles were computed with Brice's codes [12] using LSS electronic stopping. In this connection it should be noted that the position of the peaks in both types of theoretical profiles, based on Ziegler's [16] compilation of the He stopping powers in nickel are at depths closer to the surface. A similar, but larger difference between the peaks in theoretical range profiles (computed with Brice's codes and LSS electronic stopping) and the experimental swelling distributions, was observed for nickel implanted at 500°C with 20-keV ^4He ions to a dose of 2.9 x 10^{21} ions/m^2 [14]. Here, the peak swelling occurred in a depth interval that extended from 50 to 90% deeper than the calculated average projected range for 20-keV $^4He^+$ ions. Similar discrepancies have also been observed by other authors for entirely different projectile-target combinations [6,8]. The authors speculate that the differences between the theoretical peak positions and the experimentally observed peak swelling locations are mainly due to inaccurate electronic stopping power values as has also been suggested by Narayan et al. [6] and Whitley [8]. Inaccurate nuclear stopping powers would also contribute to these discrepancies , however, their relative contributions are small when compared to those of electronic stopping to the total stopping power.

For the data presented in this paper, the calculated peak in the energy deposited into damage occurs at ∿ 0.95 μm assuming theoretical LSS electronic stopping. This underestimates the peak swelling position by 0.15 to 0.25 μm. However, a shift of 0.15 to 0.25 μm in these regions can change the swelling by more than 300% as can be seen in Fig. 3(d) for nickel implanted with 500-keV He^+ ions to a dose of 1 x 10^{21} ions/m^2. It is often desirable to correlate swelling data with dpa's, however, the use of correct dpa-values for such a correlation is necessary. For example, the calculated peak energy deposited into damage (∿2 eV/A) occurs at a depth of ∿ 0.95 μm for 500-keV He ions in nickel. If one reduces the electronic stopping by 15%, the theoretical peak shifts to ∿ 1.09 μm which corresponds to the experimental peak swelling depth for the case shown in Fig. 3(a). The energy deposited into damage at

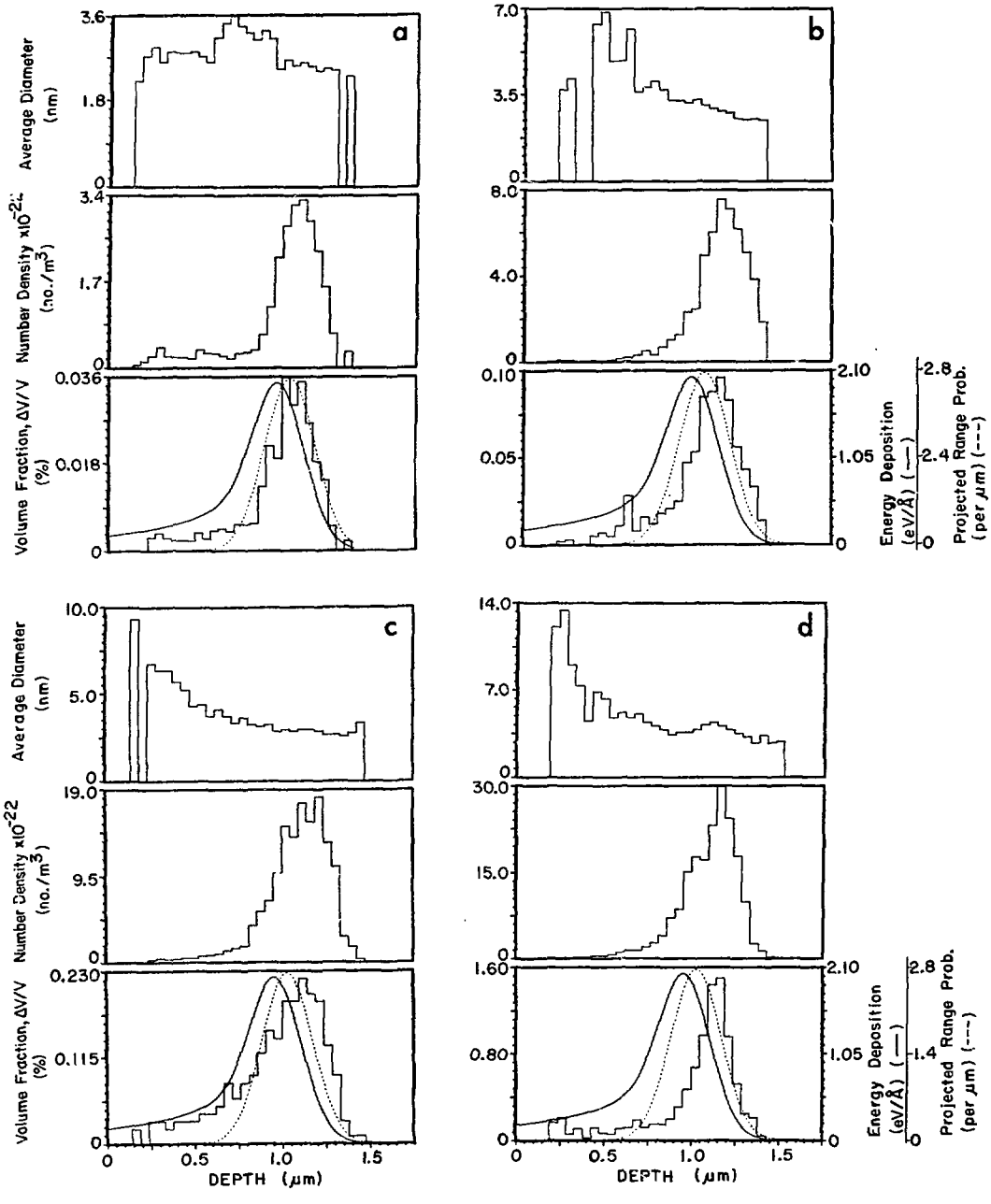

Fig. 3: The average diameter, number density, and volume fraction of cavities as a function of depth in nickel implanted at 500°C with 500-keV $^4He^+$ ions to doses of a) 2 x 10^{19} ions/m^2, b) 1 x 10^{20} ions/m^2, c) 5 x 10^{20} ions/m^2 and d) 1 x 10^{21} ions/m^2. The plots of volume fraction vs. depth include the calculated depth distribution of projected range (dashed curve) and energy deposited into damage (solid curve).

Table I. The dose dependence of cavity parameters at peak swelling depth for nickel irradiated at 500°C.

Dose (ions/m^2)x10^{20}	Peak Helium Concentration (at. %)	Peak DPA	Average Diameter (nm)	Number Density (no./m^3)x10^{22}	Volume Fraction (%)
0.2	0.06	0.04	2.5 ± 0.5	3.2	0.04
1.0	0.3	0.22	2.8 ± 0.5	7.6	0.10
5.0	1.5	1.10	3.0 ± 0.5	17.5	0.22
10.0	3.0	2.20	4.1 ± 0.5	29.9	1.50

0.95 μm decreases to a value of ∿ 1.5 eV/A; thus the dpa value is overestimated by ∿ 33% using the theoretical LSS electronic stopping.

Table 1 lists calculated peak helium concentrations and peak dpa values. The dpa's were calculated with a modified Kinchin-Pease expression assuming an efficiency factor of 0.8 and a displacement energy of 40 eV. These values are based on energy deposition profiles calculated with a 15% reduction in the LSS electronic stopping. This reduction decreases the peak value of the energy deposited into damage by ∿ 15%. Based on the peak dpa value alone, the volume swelling values for 0.22 and 1.1 dpa are in relatively good agreement with data by Packan et al. [17] for neutron irradiated nickel at 500°C, who give values of 0.2% and 0.24% at 0.5 and 0.6 dpa, respectively. Additional results by Packan et al. [17] for nickel irradiated at 500°C by Ni ions with and without helium injection indicate that the volume swelling, as well as the size and number density depend not only on the total dpa, but also on the dpa rate, the presence of helium, and whether the helium was preinjected or simultaneously injected.

Furthermore, it should be pointed out that the results reported in this paper as well as those in ref. 14 indicate that the observed discrepancy between blister skin thicknesses and the peak in calculated projected range profiles may in part be due to inaccurate electronic stopping power values, especially for energies of 20 keV or below where there exists little experimental data on stopping powers. Finally, it should be mentioned that work is in progress to determine the cavity size, number density, and swelling for doses larger than 1 x 10^{21} ions/m^2 to determine if at higher doses bubble coalescence occurs.

In conclusion, this paper presents the first quantitative results on the depth distribution of cavity size, density, and swelling of nickel irradiated at 500°C with 500-keV He^+ ions. These data reveal that the average cavity diameter, number density, and volume swelling increase with increasing dose for the dose range studied. The peak in the measured swelling distribution occurs at depths 8 to 15% larger than theoretical estimates of the projected range. These studies illustrate the need for more accurate stopping power values for the interpretation of ion induced radiation damage and blistering results.

*Work performed under the auspices of the U.S. Dept. of Energy, Div. of Basic Energy Sciences.

This paper is dedicated to the memory of Dr. Victor M. Gusev, Kurchatov Institute, Moscow.

REFERENCES

[1] M. Kaminsky and S.K. Das, Radiation Blistering-Recent Developments, invited paper presented at IX Summer School & Symp. on Physics of Ionized, Gases, Dubrovnik, Yugoslavia (1978).
[2] G.J.Thomas and W.Bauer, Nucl.Metall. 18 (1973) 255.
[3] D.J. Mazey, B.B. Eyre, J.H. Evans, S.H. Erents and G.M. McCracken, J. Nucl. Mat. 64 (1977) 145.
[4] K. Ehrlich and D. Kaletta, Radiation Effects and Tritium Technology for Fusion Reactors, CONF-750989,Vol.II (1975) 289.
[5] G.Fenske, S.K. Das and M.Kaminsky, accepted for publication in J. Nucl. Mat.
[6] J. Narayan, O.S. Oen and T.S. Noggle, J. Nucl. Mat. 71 (1977) 160.
[7] D.W. Keefer and A.G. Pard, J. Nucl. Mat. 47 (1973) 97.
[8] J.B. Whitley, Ph.D. Thesis, Univ. Wisc.-Madison (1978).
[9] C.H. Henager, J.L. Brimhall, E.P. Simonen, *Rad. Eff. 36 (1978) 49.*
[10] J.E. Harbottle, Phil. Mag. 27 (1973) 147.
[11] J.J. Laidler and F.A. Garner, Consultant Symp. on the Physics of Irradiation-Produced Voids, Sept. 9-11, 1974, AERE Rep. No. R-7934.
[12] D.K. Brice, Ion Implantation Range and Energy Deposition Codes COREL, RASE4 and DAMG2. SAND75-0622 (1977).
[13] J. Lindhard and M. Scharff, Phys. Rev. 124 (1961) 128.
[14] G. Fenske, S.K. Das, M.Kaminsky and G. H. Miley, J. Nucl. Mat. 76 & 77 (1978) 247.
[15] S.K. Das, G. Fenske and M. Kaminsky, Electron Microscopy (1978) Vol. 1, 398.
[16] J.F. Ziegler, Helium Stopping Powers and Ranges in All Elements (Pergamon Press NY 1977).
[17] N.H. Packan, K. Farrell and J.O. Stiegler, J. Nucl. Mat. 78 (1978) 143.